Strategic Synthesis of Trimetallic Au@Pd@Pt Core−Shell Nanoparticles from Poly(vinylpyrrolidone)-Based Aqueous Solution toward Highly Active Electrocatalysts

Liang Wang[†] and Yusuke Yamauchi*,[†,‡,§]

[†]World Premier International (WPI) Research Center for Materials Nanoarchitectonics (MANA), National Institute for Materials Science (NIMS), 1-1 Namiki, Tsukuba 305-0044, Japan
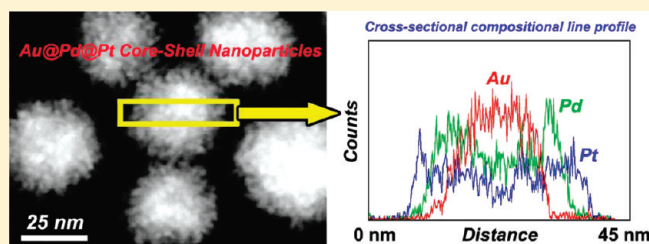
[‡]Faculty of Science & Engineering, Waseda University, 3-4-1 Ohkubo, Shinjuku, Tokyo 169-8555, Japan

[§]Precursory Research for Embryonic Science and Technology (PRESTO), Japan Science and Technology Agency (JST), 2-1 Hirosawa, Wako, Saitama 351-0198, Japan

S *Supporting Information*

ABSTRACT: Our recent study has shown that Pluronic F127 triblock copolymer can assist the formation of unique Au@Pd@Pt triple-layered core−shell-structured nanoparticles consisting of a Au core, a Pd inner layer, and nanoporous Pt outer shell (*J. Am. Chem. Soc.* **2010**, *132*, 13636). Pluronic F127 is a very typical surfactant that is commonly used in the synthesis of mesoporous silica and carbon, but Pluronic F127 is very rarely used for the synthesis of metallic nanostructures. Herein, we expand our previous concept to further demonstrate

that such interesting Au@Pd@Pt nanoparticles can be easily synthesized by using poly(vinylpyrrolidone) (PVP) instead of Pluronic F127. PVP is a very typical capping and structure-directing agent used for the synthesis of various metallic nanostructures. The present synthetic route using a PVP-based aqueous solution will greatly contribute to the further design of multilayered metallic nanoarchitectures with designed compositions and desired functions. Furthermore, a detailed investigation on the electrocatalytic activity of the trimetallic nanoparticles is also performed.

KEYWORDS: gold, palladium, platinum, nanoparticles, poly(vinylpyrrolidone), electrocatalysts

1. INTRODUCTION

The rational design of Pt-based catalysts is of considerable interest because of their unique catalytic properties.[1−6] In view of the strong social demand and the costliness of using Pt, the creation of a high-performance Pt catalyst with low cost is extremely important. The engineering of the size, shape, and composition of Pt-based materials at nanoscale can lower the Pt loading and provide more active sites, thus favoring an improved utilization efficiency and an enhanced catalytic performance.[7]

So far, several types of important Pt nanostructures (e.g., nanospheres,[8] nanofibers,[9] nanowires,[10] and so on[11−14]) have been successfully prepared. Template approaches and templateless routes are two general methods for the synthesis of Pt nanostructures with controlled size and shape. For instance, Pt nanostars can be prepared by a seed-mediated growth method using tetrahedral Pt nanocrystals as seeds,[15] and Pt nanotubes with mesoporous walls can be produced by utilizing a dual-template strategy.[16] Despite the above successful demonstrations, it is noted that the requisite multiple steps, high reaction temperature, and long duration complicate the synthetic procedures, thus making them very difficult to scale up. The development of a facile and efficient strategy to produce Pt catalysts with high activity and in high yield and large quantities is still highly desired.

In recent pioneer studies, it has been demonstrated that bimetallic catalysts show superior catalytic properties, which are not attainable by their monometallic counterparts, providing attractive perspectives for the effective tuning of the catalytic performance.[17−25] Core−shell nanostructures with designed compositions represent a highly interesting class of catalysts.[26,27] By manipulation of its compositions and/or structural features, the catalytic performance can be effectively tuned.[5a,28−30] The cases of Pt-based core−shell nanostructures are particularly interesting because of their excellent catalytic activities. For instance, Au@Pt[31] and Pd@Pt[32,33] core−shell-structured nanoparticles showed higher activities for oxygen reduction reaction than Pt nanoparticles alone. Despite the impressive advances in the design of multicomposition core−shell-structured catalyst systems, it is noted that the core−shell-structured catalysts are usually prepared by a multistep seed-mediated growth method in which the particle size and shape are uncontrollable without the use of a preformed uniform seed.[28−33] The lack of simple and direct procedures is a serious problem for large-scale synthesis as social
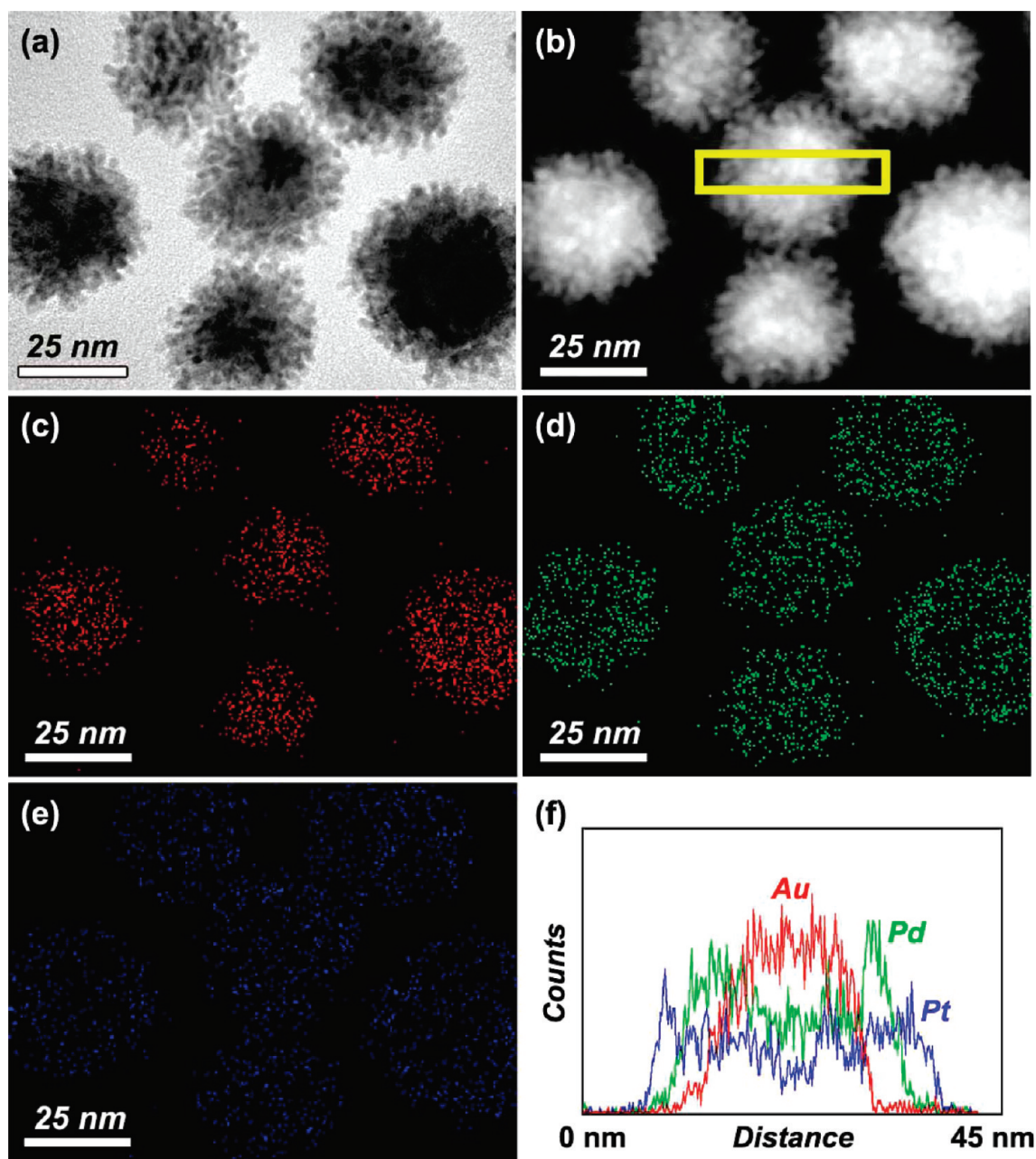
Figure 1. (a) Bright-field and (b) dark-field TEM images of Au@Pd@Pt triple-layered core—shell-structured nanoparticles. Nanoscale elemental mappings of (c) Au, (d) Pd, and (e) Pt, respectively. (f) Elemental distribution along a single nanoparticle indicated by the square in part b.

demand. The development of a facile route for Pt-based core—shell nanoarchitectures with designed compositions and desired catalytic properties is still an urgent topic to be solved.

Here, we report a very simple, one-step, and efficient route for the synthesis of unique Au@Pd@Pt triple-layered core—shell-structured nanoparticles, consisting of a Au core, a Pd inner layer, and a nanoporous Pt outer shell, in a poly(vinylpyrrolidone) (PVP)-based aqueous solution at room temperature. Our recent study has shown that Pluronic F127 triblock copolymer [$PEO_{100}-PPO_{70}-PEO_{100}$ with PEO and PPO denoting poly(ethylene oxide) and poly(propylene oxide) chains, respectively] can assist the formation of very similar Au@Pd@Pt nanoparticles.[27] Pluronic F127 is very rarely used for the synthesis of metallic nanostructures, although it has been widely used as a typical structural-

directing agent in the general synthesis of mesoporous silica and carbon materials. Herein, we expand our previous concept to further demonstrate that Au@Pd@Pt nanoparticles can be synthesized by using PVP, which is a very typical capping and structure-directing agent for the preparation of various metallic nanostructures. The general route using a PVP-based aqueous solution reported here will greatly contribute to the further design of multilayered metallic nanoarchitectures with various compositions and functions.

2. EXPERIMENTAL SECTION

2.1. Materials. $HAuCl_4$, K_2PtCl_4, Na_2PdCl_4, ascorbic acid (AA), and poly(vinylpyrrolidone) (PVP; K-30, $M_w = 40\,000$) were purchased from Nacalai Tesque Inc. (Kyoto, Japan).
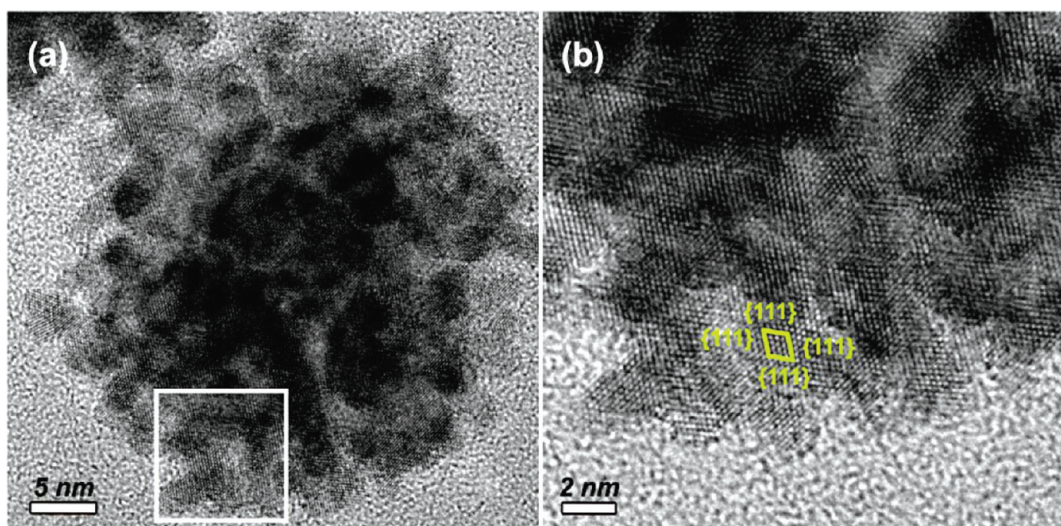
Figure 2. (a) Highly magnified TEM image of one Au@Pd@Pt triple-layered core—shell-structured nanoparticle. (b) HRTEM image of the square area in part a.

2.2. Synthesis of Au@Pd@Pt Triple-Layered Nanoparticles. In a typical synthesis of Au@Pd@Pt triple-layered nanoparticles, an aqueous precursor solution (9.0 mL) was prepared by mixing 20 mM HAuCl$_4$ (2.5 mL), 20 mM Na$_2$PdCl$_4$ (2.5 mL), 20 mM K$_2$PtCl$_4$ (2.5 mL), and PVP (0.1 g). Then, 1 mL of a 0.4 M AA solution was quickly added under sonication, giving the final HAuCl$_4$, Na$_2$PdCl$_4$, and K$_2$PtCl$_4$ precursor amounts of 0.05, 0.05, and 0.05 mmol, respectively. After being sonicated for 5 min, the mixture solution was placed for 6 h at room temperature. After the reaction was finished, the obtained product was collected by centrifugation at 10 000 rpm for 20 min and then residual PVP was removed by consecutive washing/centrifugation cycles. The collected product was dried and/or redispersed in water under sonication to produce a colloidal suspension for further characterizations.

2.3. Characterizations. Transmission electron microscopy (TEM) and high-resolution TEM (HRTEM) characterizations were carried out using a JEOL JEM-2100F operated at 200 kV equipped with energy-dispersive spectrometry analyses. The samples for TEM and HRTEM characterizations were prepared by depositing a drop of the diluted colloidal suspension on a carbon-coated copper grid. A nitrogen adsorption—desorption isotherm was obtained using a Belsorp 28 apparatus (Bel Japan, Inc.) at 77 K. The powdery sample was degassed at 60 °C for 48 h before measurement. A wide-angle powder X-ray diffraction (XRD) pattern was recorded with a Rigaku Rint 2500 diffractometer with monochromated Cu Kα radiation.

2.4. Electrochemical Investigations. Cyclic voltammograms and chronoamperometric experiments were performed by using a CHI 842B electrochemical analyzer (CHI Instruments Inc., Austin, TX). A conventional three-electrode cell was used, including a Ag/AgCl (saturated KCl) electrode as the reference electrode, a Pt wire as the counter electrode, and a working electrode. The working electrode was prepared by depositing the samples on a glassy carbon electrode (GCE; 3 mm in diameter). The GCE was coated with Au@Pd@Pt, Au@Pt, or Pt nanoparticles with the same loading of 6.0 μg and dried completely at room temperature. Then, 3.0 μL of Nafion (0.20 wt %) was coated on the surface of the modified GCE and dried before electrochemical experiments. Methanol oxidation reaction (MOR) measurements were carried out in a solution of 0.5 M H$_2$SO$_4$ containing 1 M methanol at a scan rate of 50 mV s^{-1}. Current densities were normalized by the electrochemically active surface area (ECSA) for each sample. Mass current densities were normalized by the loaded Pt

amounts, which were determined by inductively coupled plasma mass spectroscopy.

3. RESULTS AND DISCUSSION

Parts a and b of Figure 1 show TEM images of the synthesized product. The product was well-dispersed as individual spherical nanoparticles and showed three-dimensional complex nanodendrites. Elemental mapping and cross-sectional compositional line profile characterizations, which are two typically accepted characterizations revealing the core—shell structures and elemental distributions of nanostructures,[34,35] were applied to investigate the obtained product. Both of the investigations revealed that the nanoparticles were triple-layered nanostructures consisting of a Au core, a Pd inner layer, and a nanodendritic Pt outer shell (Figure 1c—f). The elemental mapping analysis further revealed the Au/Pd/Pt atomic ratio to be 1/1/1. This value coincided with the original composition in the precursor solution, indicating that all of the metal salts were completely reduced by an AA solution.

The wide-angle XRD pattern showed randomly oriented face-centered-cubic (fcc) crystals (Figure S1 in the Supporting Information) in which four peaks were assigned to (111), (200), (220), and (311) facets of crystal diffraction. Owing to the lattice mismatch factor (0.77% for Pt—Pd versus 4.08% for Pt—Au),[36] it was very difficult to resolve the peaks of Pt and Pd in the XRD pattern, whereas the peaks of Au and Pt—Pd could be readily distinguished by XRD. The highly magnified TEM image of one nanoparticle (Figure 2a) further indicated that the nanoparticle exhibited a dendritic structure with highly interconnected tendrils branching in various directions. The observed *d* spacing (0.23 nm) for the adjacent fringes in the Pt outer-shell region corresponded to the (111) planes of the Pt fcc structure (Figure 2b). Thus, it was proved that the Au@Pd@Pt triple-layered nanoparticles were successfully synthesized by a simple and one-step synthesis in a PVP-based aqueous solution at room temperature. The present method with PVP will be highly valuable for the formation of interesting trimetallic nanoparticles in the future because PVP is the most typical capping agent in the synthesis of various metallic nanostructures. The amounts of
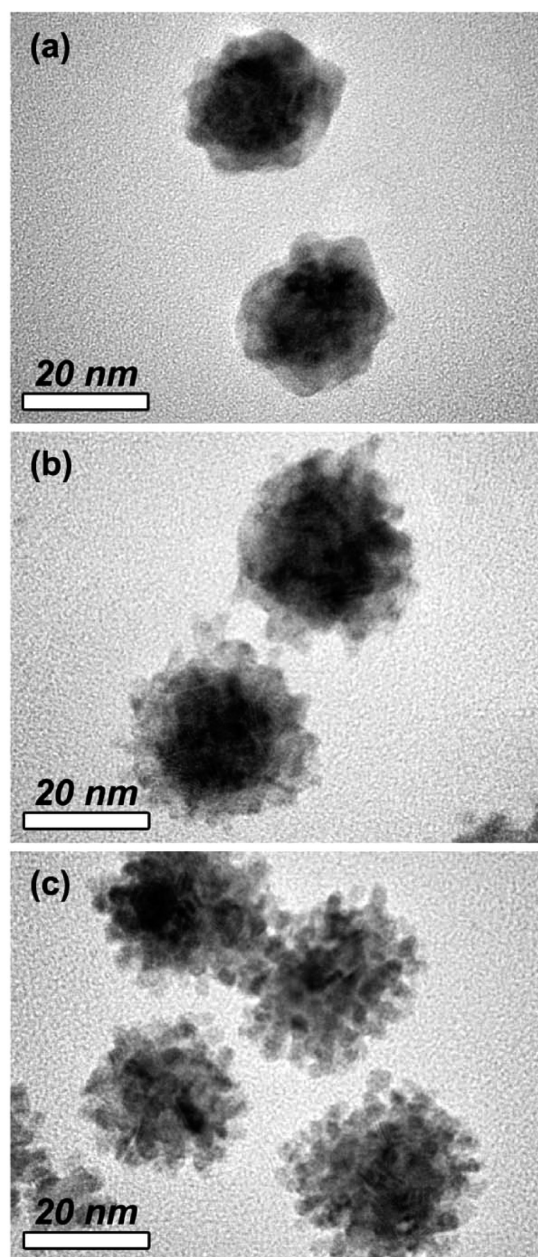
Figure 3. TEM images of the Au@Pd@Pt triple-layered core–shell-structured nanoparticles prepared from different Pt precursor amounts. The Pt precursor amounts are (a) 0.01, (b) 0.02, and (c) 0.08 mmol, respectively. The precursor amounts of Au and Pd are fixed at 0.05 and 0.05 mmol, respectively.

Figure 4. TEM images of monometallic nanoparticles (a) Au, (b) Pd, and (c) Pt, respectively, prepared by the typical synthetic procedure. For the synthesis of monometallic nanoparticles, Au (0.05 mmol), Pd (0.05 mmol), and Pt (0.05 mmol) precursors are used for the synthesis of Au, Pd, and Pt nanoparticles, respectively.

PVP are critical for the high-quality formation of the Au@Pd@Pt triple-layered nanoparticles. In the presence of sufficient PVP (e.g., 0.1 or 0.2 g in the precursor solution), high-yield synthesis was achieved. However, when the amounts of PVP were reduced (e.g., 0.01 g in the precursor solution), irregular Pt clusters were deposited in a highly aggregated form because of the absence of sufficient capping agent.

It was importantly noted that the Pt outer shell was in an interconnected tendril form. The interconnected Pt tendrils provided nanoporosity in the outer-shell regions, which were very favorable for improvement of the active surface area as catalysts. The present synthetic route could be readily scaled up
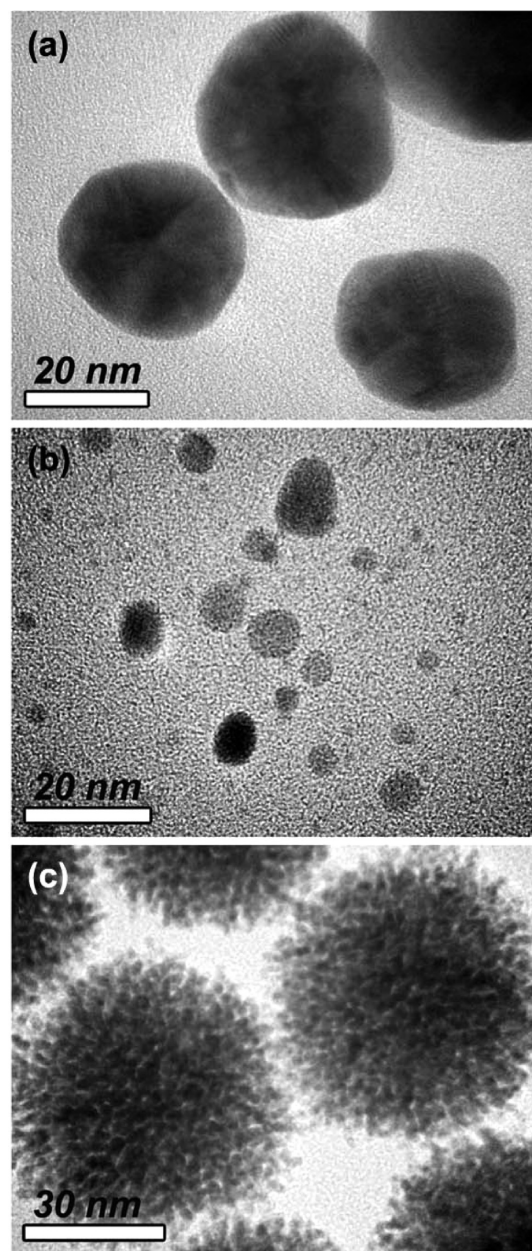
to provide enough of the sample for N_2 adsorption analysis. The obtained nanoparticles showed a specific surface area of 26 ± 2.0 m^2 g^{-1} (Figure S2 in the Supporting Information). This value was lower than that of our previous sample (31 m^2 g^{-1}) prepared with Pluronic F127,[27] probably because the thicknesses in the dendritic Pt region decreased by using a smaller amount of the Pt source. It is further noted that this value is comparative to that of the commercial Pt catalyst (JM HiSPEC 1000; surface area = $\sim$22 m^2 g^{-1}) and higher than that of the porous Pt nanoparticles prepared by using a complicated organic-phase synthesis (14 m^2 g^{-1}).[37] Branching out was a promising strategy to improve the specific surface area of the catalysts.[38] To date, the
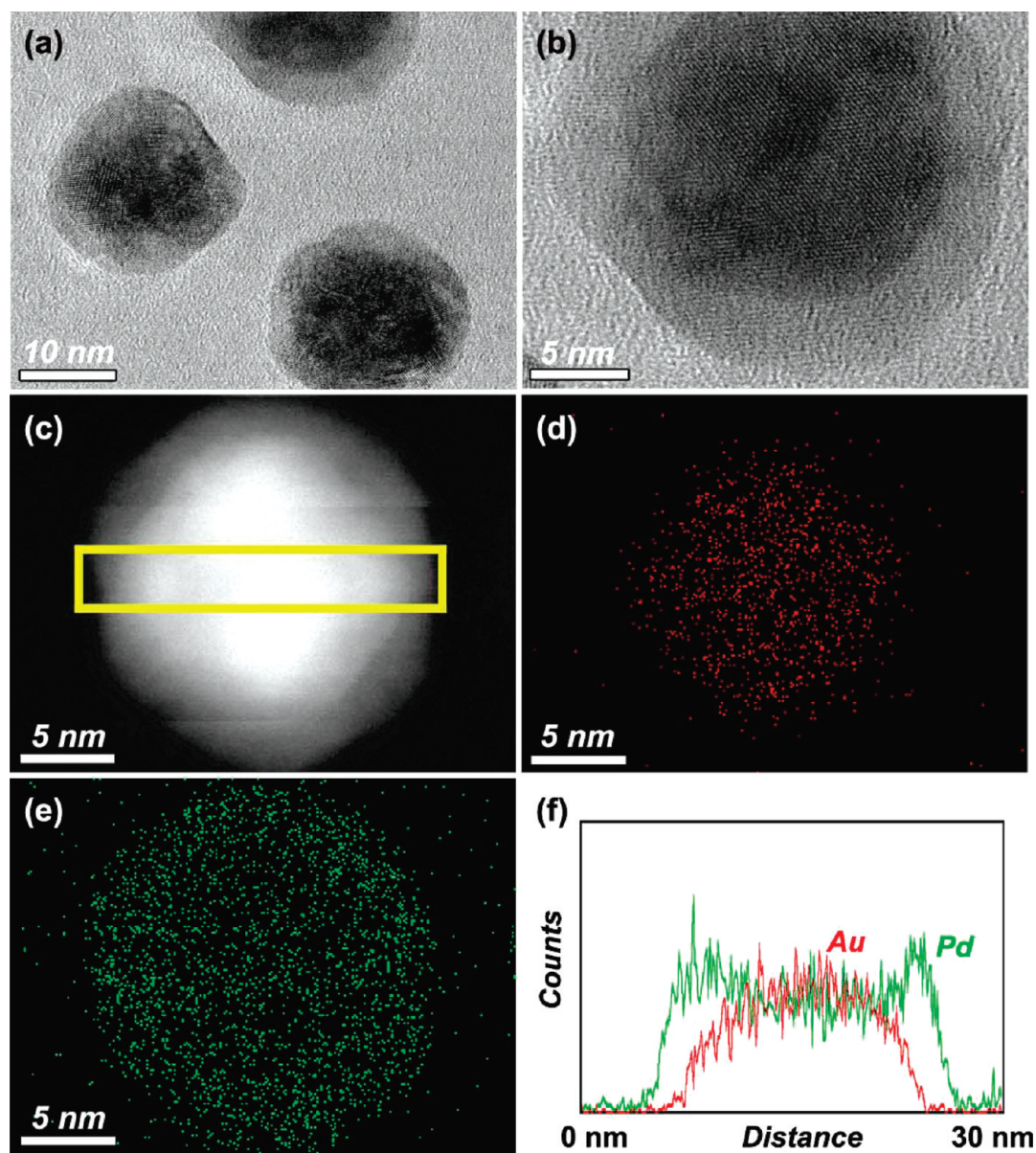
Figure 5. (a and b) Bright-field and (c) dark-field TEM images of the Au—Pd nanoparticles. The Au—Pd nanoparticles are prepared by using binary Au (0.05 mmol) and Pd (0.05 mmol) precursors. (d and e) Nanoscale elemental mappings of (d) Au and (e) Pd, respectively. (f) Elemental distribution along the area in part c.

creation of nanoporous shells onto metal-based cores has been reported, but the compositions were very limited to only silica and carbon.[39,40] The creation of metallic nanoporous shells is important for the development of highly active catalysts. The rich edges and corner atoms derived from the tendril Pt architectures are highly valuable for enhancement of the Pt catalytic activity.[15,41]

The configuration of the Pt outer shell could be effectively tuned simply by controlling the amount of the Pt precursor in the reactive bath (Figure 3). When the Pt precursor amount was decreased to 0.01 mmol, the Pt outer shells appeared to be near smooth. With an increase of the Pt precursor amount to 0.02 mmol, the tendril Pt architectures were observed. A further increase of the Pt precursor amount from 0.05 to 0.08 mmol led to the presence of dentritic Pt nanoparticles without cores as a byproduct. Facile controls of the Pt outer shell were valuable for tuning the catalytic property.

To help understand the formation mechanism of the interesting Au@Pd@Pt triple-layered nanostructures, a detailed investigation was performed in which monometallic precursors (Au, Pd, and Pt, respectively) and bimetallic precursors (Au—Pd, Au—Pt, and Pd—Pt, respectively) were reduced under the same synthetic procedure, respectively. The shapes of the monometallic Au, Pd, and Pt nanoparticles were near spherical, ultrafinely spherical, and dendritic, respectively (Figure 4), revealing that PVP was favorable for spherical growth of Au and Pd nanoparticles and facilitated the formation of dendritic Pt nanoparticles in the present reaction system. The reduction of Au—Pd and Au—Pt binary precursors led to the formation of Au@Pd core—shell nanoparticles with a smooth Pd shell (Figure 5) and Au@Pt core—shell particles with a nanodendritic Pt shell (Figure 6), respectively, whereas when deposition of the Pd—Pt binary precursors was conducted (Figure S3 in the Supporting Information), irregular nanoparticles were
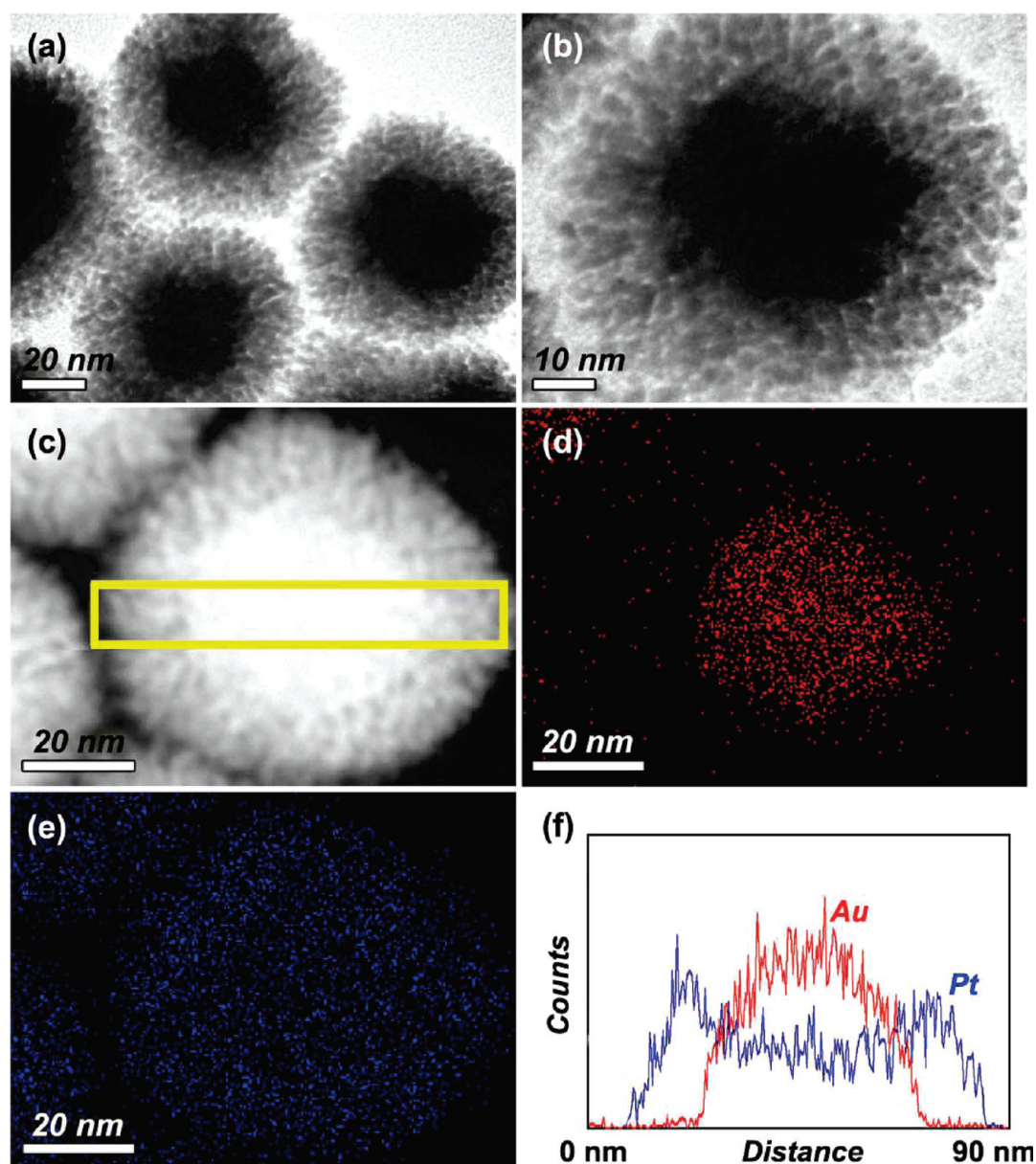
Figure 6. (a and b) Bright-field and (c) dark-field TEM images of the Au—Pt nanoparticles. The Au—Pt nanoparticles are prepared by using binary Au (0.05 mmol) and Pt (0.05 mmol) precursors. (d and e) Nanoscale elemental mappings of (d) Au and (e) Pt, respectively. (f) Elemental distribution along the area in part c.

obtained. On the basis of the bimetallic system investigations, it was known that the reduction of the Au precursor was preferentially performed over those of the Pd and Pt precursors in the reactive system and then the Au nanoparticles severed as seeds for the subsequent deposition of Pt and Pd layers. The presence of a Au seed was critical for the formation of the core—shell structures. In the absence of Au species, it was very difficult for depositions of Pt and Pd to spontaneously form core—shell structures (Figure S3 in the Supporting Information).

To further elucidate the formation process of the Au@Pd@Pt nanoparticles, three intermediate products sampled at different reaction times were characterized by TEM (Figure 7). TEM investigations displayed that the Au@Pd core—shell nanoparticles were initially formed, and then the Pd shell grew, and finally the dendritic Pt outer shell was deposited onto the surface of the Pd layer. During the Pt deposition, PVP facilitated the formation

of the dendritic Pt outer shell (Figure 4c).[42] On the basis of the above observation, it was further clarified that the formation of the Au@Pd@Pt triple-layered nanostructure was triggered by the initial formation of spherical Au nanoparticles. The Au nanoparticles that were formed at the early stage of reaction truly serve as the seed for subsequent depositions of the Pd inner layer and Pt outer shell. The spontaneous separation of the formation of the Au core, Pd inner layer, and Pt outer shell was thought to occur as a result of the different reduction kinetics.

The rational use of spontaneous separations of the depositions of different metals is a highly useful concept for the one-step formation of core—shell bimetallic nanostructures. In the previous works by others, two papers on the one-step formation of Au@Pd[43] and Au@Co[26] core—shell bimetallic nanoparticles have been reported, to the best of our knowledge. However, the shell regions in the previous products (Au@Pd[43] and
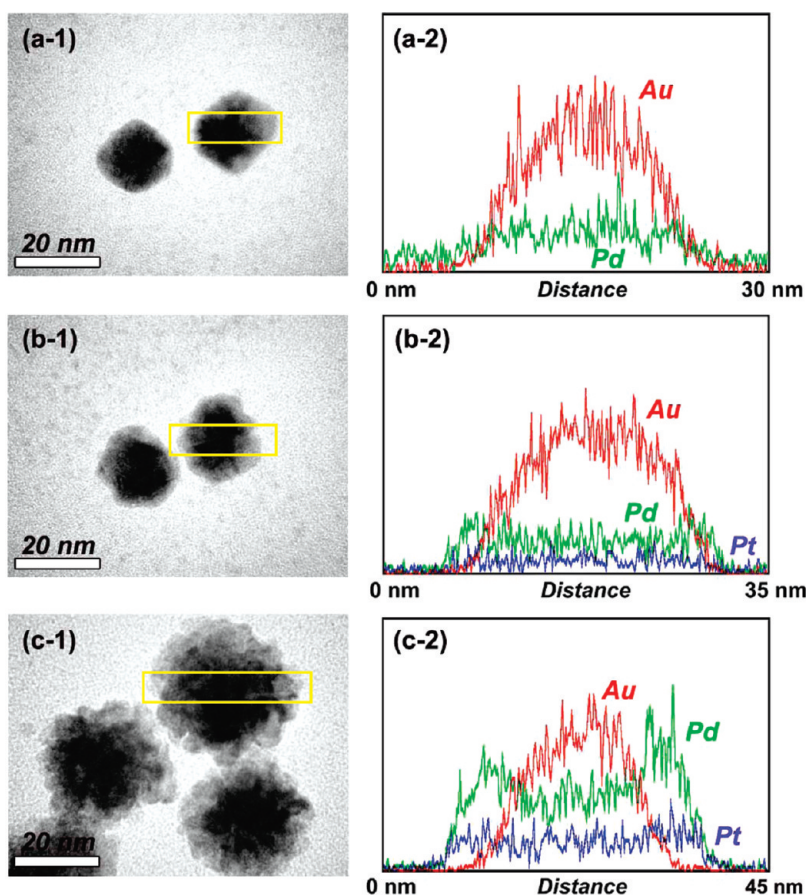
Figure 7. Time-dependent TEM images of the Au@Pd@Pt triple-layered core–shell-structured nanoparticles. (a-1, b-1, and c-1) Bright-field TEM images of the intermediate products sampled at different reaction periods [(a) 30 s, (b) 3 min, and (c) 30 min]. (a-2, b-2, and c-2) Elemental distributions along the areas indicated by the squares.
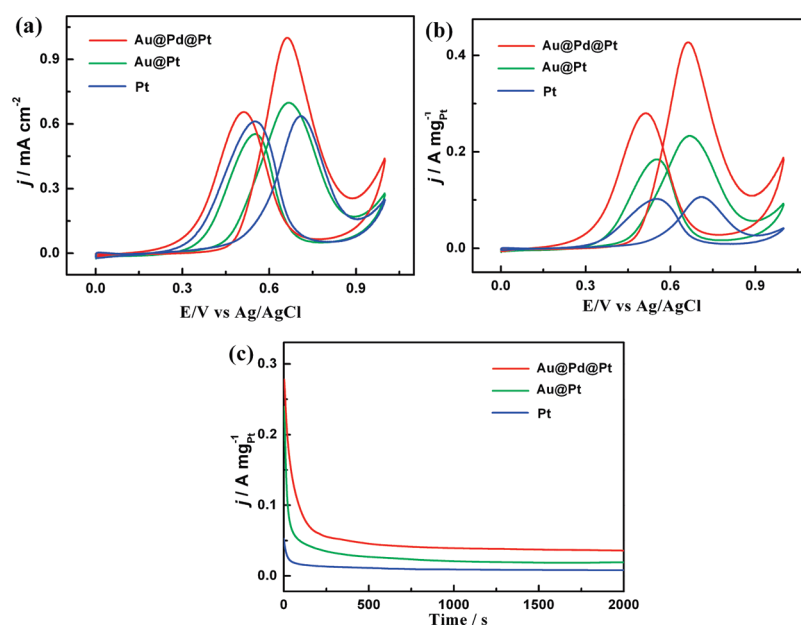

Figure 8. (a and b) CV and (c) CA curves for MORs catalyzed by (red) Au@Pd@Pt nanoparticles, (green) Au@Pt nanoparticles, and (blue) dendritic Pt nanoparticles, respectively, in 0.5 M H_2SO_4 with 1 M methanol. Chronoamperometric curves are recorded at 0.6 V.

Au@Co[26] core—shell nanoparticles) have no nanoporosity, resulting in the difficulty for guest species to access the inner cores. This fact seriously devalues the advantages of the core—shell architectures. Our synthesis reported herein is favorable for creating nanoporous Pt outer shell, thereby expecting the integrated functionalities derived from both the core and shell.

Inspired by its attractive architectures (e.g., core—shell structure with a nanoporous Pt outer shell) and fascinating properties (e.g., high surface area), the Au@Pd@Pt triple-layered nanoparticles (as displayed in Figure 1) were explored as catalysts for MORs. The electrocatalytic performance was evaluated by cyclic voltammetry (CV) and chronoamperommetry (CA) investigations in a 0.5 M H_2SO_4 aqueous solution in the presence of 1 M methanol at room temperature. For comparison, the Au@Pt nanoparticles (with a Au core and dendritic Pt shell, as shown in Figure 6) and dendritic Pt nanoparticles (as displayed in Figure 4c) were also tested. The CV and CA current densities were normalized by ECSA (specific activity) and by Pt mass (mass activity), respectively, and the results are displayed in Figure 8.

As shown in Figure 8, the observed voltammetric feature for the MOR catalyzed by the Au@Pd@Pt triple-layered nanoparticles was consistent with the ones obtained by Au@Pt and Pt nanoparticles. The catalytic peak current density of the Au@Pd@Pt triple-layered nanoparticles in the positive direction sweep (1.02 mA cm^{-2}) was about 1.5 times higher than that of the Au@Pt nanoparticles (0.68 mA cm^{-2}) and about 1.6 times higher than that of the Pt nanoparticles (0.63 mA cm^{-2}) (Figure 8a), while its mass peak current density (0.43 A mg$_{Pt}$$^{-1}$) was about 1.9 times higher than that of the Au@Pt nanoparticles (0.23 A mg$_{Pt}$$^{-1}$) and about 3.9 times higher than that of the Pt nanoparticles (0.11 A mg$_{Pt}$$^{-1}$) (Figure 8b). These results indicated that the Au@Pd@Pt triple-layered nanoparticles showed higher electrocatalytic activity than those of the Au@Pt and dendritic Pt nanoparticles in terms of both the specific activity and mass activity. The superior catalytic properties of the Au@Pd@Pt triple-layered nanoparticles were comparable or higher than those reported in Pt-based catalysts[44] and notably higher than those of commercial Pt black (PB)[44b,e] and commercial E-TEK Pt/C catalysts.[44b,d] CA curves recorded at 0.6 V for 2000 s (Figure 8c) indicated that the current densities of the Au@Pd@Pt triple-layered nanoparticles were higher than those of the Au@Pt and dendritic Pt nanoparticles in the entire time range, which further testified to a superior stability in MORs.

All of the three catalysts (i.e., Au@Pd@Pt triple-layered nanoparticles, Au@Pt core—shell nanoparticles, and dendritic Pt nanoparticles) possessed dendritic and nanoporous Pt surfaces, which offered active Pt sites (rich edges and corner atoms) for methanol dissociation, thus facilitating the MOR.[21] Also, it is well-known that Pt—Pd alloys show higher catalytic activity than Pt alone.[22] Considering the high degree of lattice match of Pt—Pd (99.23%), the Pd atoms in the inner layer of the Au@Pd@Pt triple-layered nanoparticles are though to be matched with the lattice structure of the Pt atoms in the outer layer, meaning that a pseudo Pd—Pt alloy is probably formed at the interface between the Pd and Pt layers.[45] The pseudoalloying of Pt with Pd is favorable for reducing the electronic binding energy in Pt, thereby facilitating the C—H cleavage reaction in methanol decomposition.[21] Therefore, in the present study, during the MOR, methanol species readily accessed the pseudo inserted Pd—Pt alloy through the nanoporous Pt outer shell with high permeability. Then, the pseudo inserted Pd—Pt alloy could serve as higher catalytic sites. The Au core was protected by the nonporous Pd inner layer, and thus the methanol species could not access the Au core during the MOR process. This meant that the Au core severed as only the seed for subsequent depositions of the Pd inner layer and Pt outer shell, as was already discussed above. Thus, through control of the compositions and structures, a remarkably enhanced catalytic activity was realized.

4. CONCLUSION

We have successfully synthesized Au@Pd@Pt triple-layered nanoparticles with a Au@Pd bimetallic core and a nanoporous Pt shell by a simple one-step aqueous-phase reaction at room temperature. The obtained Au@Pd@Pt triple-layered nanoparticles displayed a drastically enhanced catalytic activity for MORs, demonstrating its promising potential as an effective catalyst. The proposed one-step synthesis is quite unique in its simplicity and can be scaled up readily. The developed facile route is highly valuable and feasible for routinely producing Pt-based catalysts with highly catalytic active sites for commercial devices. The unique nanoarchitectures with designed structural features and compositions are scientifically and technologically important and have great potential in energy science beyond fuel cell catalysts, such as hydrogen storage,[45] and so on. The effort reported here will inspire the further design of multilayered metallic nanoarchitectures in the future.

■ ASSOCIATED CONTENT

ⓢ **Supporting Information.** Additional characterization data (PDF). This material is available free of charge via the Internet at http://pubs.acs.org.

■ AUTHOR INFORMATION

Corresponding Author
*E-mail: Yamauchi.Yusuke@nims.go.jp.

■ ACKNOWLEDGMENT

■ REFERENCES

(1) Li, Y.; Somorjai, G. A. *Nano Lett.* **2010**, *10*, 2289–2295.

(2) Lee, S. W.; Chen, S.; Sheng, W.; Yabuuchi, N.; Kim, Y.; Mitani, T.; Vescovo, E.; Shao-Horn, Y. *J. Am. Chem. Soc.* **2009**, *131*, 15669–15677.

(3) Xu, D.; Liu, Z. P.; Yang, H. Z.; Liu, Q. S.; Zhang, J.; Fang, J. Y.; Zou, S. Z.; Sun, K. *Angew. Chem., Int. Ed.* **2009**, *48*, 4217–4221.

(4) Liu, Q. S.; Yan, Z.; Henderson, N. L.; Bauer, J. C.; Goodman, D. W.; Batteas, J. D.; Schaak, R. E. *J. Am. Chem. Soc.* **2009**, *131*, 5720–5721.

(5) Liu, Z.; Jackson, G. S.; Eichhorn, B. W. *Angew. Chem., Int. Ed.* **2010**, *49*, 3173–3176.

(6) Tian, N.; Zhou, Z.; Sun, S.; Ding, Y.; Wang, Z. *Science* **2007**, *316*, 732–735.

(7) (a) Mostafa, S.; Behafarid, F.; Croy, J. R.; Ono, L. K.; Li, L.; Yang, J. C.; Frenkel, A. I.; Cuenya, B. R. *J. Am. Chem. Soc.* **2010**, *132*, 15714–15719. (b) Peng, Z.; You, H.; Wu, J.; Yang, H. *Nano Lett.* **2010**, *10*, 1492–1496. (c) Wu, J.; Zhang, J.; Peng, Z.; Yang, S.; Wagner, F. T.; Yang, H. *J. Am. Chem. Soc.* **2010**, *132*, 4984–4985.

(8) Bigall, N. C.; Hartling, T.; Klose, M.; Simon, P.; Eng, L. M.; Eychmuller, A. *Nano Lett.* **2008**, *8*, 4588–4592.

(9) Yamauchi, Y.; Takai, A.; Nagaura, T.; Inoue, S.; Kuroda, K. *J. Am. Chem. Soc.* **2008**, *130*, 5426–5427.

(10) Koenigsmann, C.; Zhou, W.; Adzic, R. R.; Sutter, E.; Wong, S. S. *Nano Lett.* **2010**, *10*, 2806–2811.

(11) Gorzny, M. Ł.; Walton, A. S.; Evans, S. D. *Adv. Funct. Mater.* **2010**, *20*, 1295–1300.

(12) Song, Y.; Dorin, R. M.; Garcia, R. M.; Jiang, Y.; Wang, H.; Li, P.; Qiu, Y.; Swol, F.; Miller, J. E.; Shelnutt, J. A. *J. Am. Chem. Soc.* **2008**, *130*, 12602–12603.

(13) (a) Wang, L.; Wang, H. J.; Nemoto, Y.; Yamauchi, Y. *Chem. Mater.* **2010**, *22*, 2835–2841. (b) Wang, L.; Hu, C. P.; Nemoto, Y.; Tateyama, Y.; Yamauchi, Y. *Cryst. Growth Des.* **2010**, *10*, 3454–3460. (c) Wang, L.; Guo, S. J.; Zhai, J. F.; Dong, S. J. *J. Phys. Chem. C* **2008**, *112*, 13372–13377.

(14) Takai, A.; Yamauchi, Y.; Kuroda, K. *J. Am. Chem. Soc.* **2010**, *132*, 208–214.

(15) Mahmoud, M. A.; Tabor, C. E.; El-Sayed, M. A.; Ding, Y.; Wang, Z. *J. Am. Chem. Soc.* **2008**, *130*, 4590–4591.

(16) Takai, A.; Yamauchi, Y.; Kuroda, K. *Chem. Commun.* **2008**, *44*, 4171–4173.

(17) Peng, Z.; Yang, H. *Nano Today* **2009**, *4*, 143–164.

(18) Chen, A.; Holt-Hindle, P. *Chem. Rev.* **2010**, *110*, 3767–3804.

(19) Wang, J.; Asmussen, R. M.; Adams, B.; Thomas, D. F.; Chen, A. *Chem. Mater.* **2009**, *21*, 1716–1724.

(20) Zhang, J.; Yang, H.; Fang, J.; Zou, S. *Nano Lett.* **2010**, *10*, 638–644.

(21) (a) Liu, L.; Pippel, E.; Scholz, R.; Gosele, U. *Nano Lett.* **2009**, *9*, 4352–4358. (b) Liu, L.; Scholz, R.; Pippel, E.; Gosele, U. *J. Mater. Chem.* **2010**, *20*, 5621–5627.

(22) (a) Huang, X.; Zhang, H.; Guo, C.; Zhou, Z.; Zheng, N. *Angew. Chem., Int. Ed.* **2009**, *48*, 4808–4812. (b) Yuan, Q.; Zhou, Z.; Zhuang, J.; Wang, X. *Chem. Commun.* **2010**, *46*, 1491–1493.

(23) Maksimuk, S.; Yang, S.; Peng, Z.; Yang, H. *J. Am. Chem. Soc.* **2007**, *129*, 8684–8685.

(24) Kim, J.; Lee, Y.; Sun, S. *J. Am. Chem. Soc.* **2010**, *132*, 4996–4997.

(25) Wang, L.; Yamauchi, Y. *Chem. Asian J.* **2010**, *5*, 2493–2498.

(26) Yan, J.; Zhang, X.; Akita, T.; Haruta, M.; Xu, Q. *J. Am. Chem. Soc.* **2010**, *132*, 5326–5327.

(27) Wang, L.; Yamauchi, Y. *J. Am. Chem. Soc.* **2010**, *132*, 13636–13638.

(28) (a) Mazumder, V.; Chi, M.; More, K. L.; Sun, S. *J. Am. Chem. Soc.* **2010**, *132*, 7848–7849. (b) Mazumder, V.; Chi, M.; More, K. L.; Sun, S. *Angew. Chem., Int. Ed.* **2010**, *49*, 9368–9372.

(29) Wang, C.; Tian, W.; Ding, Y.; Ma, Y.; Wang, Z.; Markovic, N. M.; Stamenkovic, V. R.; Daimon, H.; Sun, S. *J. Am. Chem. Soc.* **2010**, *132*, 6524–6529.

(30) Zhou, S.; McIlwrath, K.; Jackson, G.; Eichhorn, B. *J. Am. Chem. Soc.* **2006**, *128*, 1780–1781.

(31) Kim, Y.; Hong, J. W.; Lee, Y. W.; Kim, M.; Kim, D.; Yun, W. S.; Han, S. W. *Angew. Chem., Int. Ed.* **2010**, *49*, 10197–10201.

(32) Lim, B.; Jiang, M.; Camargo, P. H. C.; Cho, E. C.; Tao, J.; Lu, X.; Zhu, Y.; Xia, Y. *Science* **2009**, *324*, 1302–1305.

(33) Peng, Z.; Yang, H. *J. Am. Chem. Soc.* **2009**, *131*, 7542–7543.

(34) (a) Fan, F.; Liu, D.; Wu, Y.; Duan, S.; Xie, Z.; Jiang, Z.; Tian, Z. *J. Am. Chem. Soc.* **2008**, *130*, 6949–6951. (b) Lim, B.; Wang, J.; Camargo, P. H. C.; Jiang, M.; Kim, M.; Xia, Y. *Nano Lett.* **2008**, *8*, 2535–2540. (c) Ferrer, D.; Torres-Castro, A.; Gao, X.; Sepúlveda-Guzmán, S.; Ortiz-Méndez, U.; José-Yacamán, M. *Nano Lett.* **2007**, *7*, 1701–1705.

(35) Wang, D.; Li, Y. *J. Am. Chem. Soc.* **2010**, *132*, 6280–6281.

(36) Habas, S. E.; Lee, H.; Radmilovic, V.; Somorjai, G. A.; Yang, P. *Nat. Mater.* **2007**, *6*, 692–697.

(37) Teng, X.; Liang, X.; Maksimuk, S.; Yang, H. *Small* **2006**, *2*, 249–253.

(38) Wang, L.; Yamauchi, Y. *J. Am. Chem. Soc.* **2009**, *131*, 9152–9153.

(39) (a) Deng, Y.; Cai, Y.; Sun, Z.; Liu, J.; Liu, C.; Wei, J.; Li, W.; Liu, C.; Wang, Y.; Zhao, D. *J. Am. Chem. Soc.* **2010**, *132*, 8466–8473. (b) Deng, Y.; Qi, D.; Deng, C.; Zhang, X.; Zhao, D. *J. Am. Chem. Soc.* **2008**, *130*, 28–29. (c) Joo, S. H.; Park, J. Y.; Tsung, C. K.; Yamada, Y.; Yang, P.; Somorjai, G. A. *Nat. Mater.* **2009**, *8*, 126–131. (d) Arnal, P. M.; Schüth, F.; Kleitz, F. *Chem. Commun.* **2006**, 1203–1205.

(40) Ikeda, S.; Ishino, S.; Harada, T.; Okamoto, N.; Sakata, T.; Mori, H.; Kuwabata, S.; Torimoto, T.; Matsumura, M. *Angew. Chem., Int. Ed.* **2006**, *45*, 7063–7066.

(41) Lim, B.; Lu, X.; Jiang, M.; Camargo, P. H. C.; Cho, E. C.; Lee, E. P.; Xia, Y. *Nano Lett.* **2008**, *8*, 4043–4047.

(42) Wang, L.; Yamauchi, Y. *Chem. Mater.* **2009**, *21*, 3562–3569.

(43) Lee, Y.; Kim, M.; Kim, Z. H.; Han, S. W. *J. Am. Chem. Soc.* **2009**, *131*, 17036–17037.

(44) (a) Lee, E. P.; Peng, Z.; Chen, W.; Chen, S.; Yang, H.; Xia, Y. *ACS Nano* **2008**, *2*, 2167–2173. (b) Guo, S.; Dong, S.; Wang, E. *ACS Nano* **2010**, *4*, 547–555. (c) Ataee-Esfahani, H.; Wang, L.; Nemoto, Y.; Yamauchi, Y. *Chem. Mater.* **2010**, *22*, 6310–6318. (d) Guo, S.; Dong, S.; Wang, E. *Chem. Commun.* **2010**, *46*, 1869–1871. (e) Guo, S.; Li, J.; Dong, S.; Wang, E. *J. Phys. Chem. C* **2010**, *114*, 15337–15342.

(45) Yamauchi, M.; Kobayashi, H.; Kitagawa, H. *ChemPhysChem* **2009**, *10*, 2566–2576.